International Journal of Technology

http://ijtech.eng.ui.ac.id

Research Article

Improving Fire Extinguishing Properties of Class B Fire with Cellulose-Hydrogel from Water Hyacinth (*Eichhornia crassipes*) Extract

Surachat Sinworn [1], Nuttabodee Viriyawattana [1,*]

[1]*Department of Occupational Health and Safety, Faculty of Science and Technology, Suan Dusit University, Bangplad District, Bangkok, Thailand, 10700,*
[*]*Corresponding author: nuttabodee_vir@dusit.ac.th; Tel.: +66 4239429*

Abstract: Cellulose can be processed into a hydrogel that enhances performance in extinguishing Class B (oil) fire. This hydrogel has a significant increase in viscosity after exposure to high temperatures. As the temperature increases, the viscosity rises, enhancing the ability of hydrogel to coat the fuel surface and effectively prevent the production of flammable vapor. Therefore, this study aimed to synthesize cellulose-based hydrogel by extracting water hyacinth to obtain cellulose in the form of methylcellulose (MC) powder. Properties of cellulose hydrogel were tested using Fourier Transform-Infrared Spectrometer (FT-IR), Scanning Electron Microscope (SEM), Energy Dispersive X-Ray Spectroscopy (EDX), viscosity, Thermogravimetric Analysis (TGA), and gel fraction analysis. To define its performance, fire extinguishing efficiency tests were performed by comparing mono-ammonium phosphate (MAP) or ABC (control) and MAP+ cellulose hydrogel (treatment). The data obtained were the radiation temperature, the time required to extinguish fire, and characteristics of the fuel coating during combustion. The results showed that fire extinguishing performance for Class B fire, in terms of radiation temperature, was lower for MAP+cellulose Hydrogel at 284.67±39.28°C, compared to MAP at 368.10±51.46°C. Extinguishing time for the MAP+ Cellulose Hydrogel was 4.19 seconds faster than only MAP. Additionally, the coating properties improved as the substance transitioned from powder to gel, effectively coating the fuel at high temperatures. This was consistent with the results of the Gel Fraction Analysis and TGA, which prevented fire spread and improved flame retardancy.

Keywords: Cellulose hydrogel; Class B; Fire extinguisher; Water hyacinth

1. Introduction

The growth of high-rise building is triggered by expensive land prices and the need for construction of hotels, offices, and colleges. Besides the great benefits, high-rise building also has a consequence of fire risk, mostly from Class A and B fire. (Nugroho et al., 2022). This risk is often addressed by emergency protocols using portable dry chemical, containing mainly Monoammonium Phosphate ($NH_4H_2PO_4$) mixed with other compounds to make the powder slippery, non-stick, and non-clogging when sprayed. Portable dry chemical is also known as ABC Powder and is effective in extinguishing fire such as Nippon and Saturn brand, including extinguishing Class A, B, and C. The concentration of the chemical depends on fire Rating of each model. Class A includes fire from common combustibles such as wood, cloth, and paper. Class B

Science Promotion Fund Research and Innovation Fund, Thailand, Project No. 193094

https://doi.org/10.14716/ijtech.v16i2.7387
Received November 2024; Revised December 2024; Accepted January 2025

comprises fire from oils and gases, while Class C is from electricity (Viriyawattana and Sinworn, 2023).

The selection of extinguisher is commonly based on the criteria of easy access, use, and basic storage. Firefighting protocols use this extinguisher as a crucial first step in controlling an initial fire before developing into a larger uncontrollable blaze. Presently, fire extinguishing agents are required to be non-toxic and safe for humans as well as the environment (Han et al., 2020). This is in line with the Montreal Protocol, Paris Agreement, and other agreements between international organizations and countries. Currently, there is increasing demand for environmental protection, particularly for the development of circular or green economies, which focus on the quality and accessibility of sustainable raw materials, including cellulose waste. These materials are renewable sources of biomass for the ecological environment. Approximately 181.5 billion tonnes of cellulose are produced annually worldwide (Sayara and Sánchez, 2019). Cellulose is particularly targeted because it is derived from waste materials such as agricultural residues, forests, and grass. Waste materials are primarily composed of polymers found in plant cell walls, including 40-50 wt% cellulose, 15-35 wt% hemicellulose, and 20-40 wt% lignin (Yang and Lü, 2021). Cellulose derived from biomass is biodegradable and renewable, making it a suitable alternative to synthetic chemicals. This helps reduce global warming and the environmental impact of various chemicals (Varma, 2019).

Cellulose, the most abundant biomass resource, originated from plants and microorganisms such as algae and tunicate. (Harahap et al., 2023). Cellulose, a member of the polysaccharide family, is the most prevalent organic component generated from biomass (Nurhayati et al., 2024). Cellulose is the primary raw material for nanocellulose and can be used to develop products with diverse properties such as insulating materials, nanocomposites, and nanohybrids. Particularly, derivatives such as Carboxymethyl Cellulose (CMC) and Methyl Cellulose (MC) are cellulose ethers with excellent film-forming properties, serving as potential materials for fabricating films from plant-based cellulose (Rahman et al., 2021). These materials enhance the flow properties of substances in fire extinguisher by improving their compatibility, as shown in the test of the compatibility of starch-methyl mixes using oscillatory rheometry. Cellulose has also been reported to be a biocompatible polymer (Ma et al., 2008). However, fire resistance can be enhanced by transforming cellulose into nanocellulose forms, targeting the reconstruction of thin films, coatings, and aerogels (Sen et al., 2022). Cellulose exists in various forms such as derivatives, regenerated, microcrystalline cellulose (MCC), cellulose nanocrystals (CNC), cellulose nanofibrils (CNF), and other modified types (Bangar et al., 2022; Alavi, 2019). The various forms have been explored for their fire-resistant properties in thin films, coatings, and aerogels prepared from subcomponents (Jamsaz and Goharshadi, 2023; Yadav et al., 2022). Additionally, cellulose ethers are non-ionic substances, such as MC, which are widely used in water-based latex coatings and often formed into gel to retain water in powdered materials (Kibar and Us, 2014). The coating film is derived from a gel produced from MC, which primarily contains silicate.

Fire tests on various gel materials have shown that fire-extinguishing gel effectively self-inhibits combustion (Boukind et al., 2022; Shi and Zhou, 2014). MC is an intriguing smart biomaterial that forms a thermally reversible gel. When subjected to thermal stimuli, aqueous solutions containing MC at critical concentrations form stable, physically cross-linked hydrogel to modify the chemical, physical, and biomechanical properties. This thermal responsiveness plays a significant role because physiological temperatures can act as a trigger point to control properties of MC. Hydrogel is a polymer with a three-dimensional structure composed of large, cross-linked, and hydrophilic molecules (Chai et al., 2017; Ebara et al., 2014; Yuan et al., 2013). Compared to pure water, hydrogels offer superior advantages in terms of water retention, cooling, and sealing properties. Currently, hydrogel is widely used for wildfire and coal mine fire prevention (Zhang et al., 2023). Synthesized hydrogel with novel multiphase foam gels to improve fire- extinguishing performance (Shi and Qin, 2019; Qin et al., 2014; Xi et al., 2014). The material was prepared by mechanically

stirring fly ash (foaming agent), nitrogen (thickening agent), and a cross-linking agent. The gels obtained through a mechanical foaming process show excellent fire-extinguishing properties.

Chemical foaming is another effective method for advancing the porous structure into gel. The porous structure is derived from a mixture of specific chemicals that react with acids or decompose at high temperatures to produce gas. These reactions create bubbles during the polymerization process, producing a porous polymer structure (Wang et al., 2014). Kabiri et al. (2003) synthesized an effective hydrogel with excellent absorbency using acetone and sodium bicarbonate ($NaHCO_3$) as foaming agents (Kabiri et al., 2003). The results showed that gel responded immediately to temperature changes, allowing approximately 90% of water to evaporate within 10 minutes, making it an excellent cooling material for fire-damaged areas.

The hydrogel properties of cellulose have been used to enhance the effectiveness of dry chemical fire extinguisher. This enhancement is achieved by adding MC derived from water hyacinth, a prolific and problematic weed in public water bodies. The method can reduce the amount of water hyacinth, serving as a natural, non-toxic substance in the products. The additive cellulose forms a sticky film that coats the oil surface more effectively and has a low melting point, allowing quick formation. The film has the characteristics of extinguishing Class B fire, which is different from Class A made of solid materials such as wood and paper. The performance test of Mono Ammonium Phosphate (MAP) combined with Cellulose Hydrogel fire extinguisher on Class B shows higher efficiency in terms of faster extinguishing times compared to only MAP. The combination also provides better fire resistance by coating a stagnant fuel surface and creating a slim adhesive layer on the fuel surface (Evegren and Hertzberg, 2017).

Based on the description, this study aimed to investigate the preparation of hydrogel from cellulose ether extracted from water hyacinth, a natural and substantial source of cellulose. The properties of cellulose and hydrogel were evaluated using methods such as Fourier Transform Infrared Spectrometer (FT-IR), Scanning Electron Microscope (SEM), Energy Dispersive X-Ray Spectroscopy (EDX), viscosity, Thermogravimetric Analysis (TGA), and gel fraction analysis. Furthermore, fire-extinguishing performance was evaluated by comparing the performance of the MAP or ABC (control) agent with that of the ABC + cellulose hydrogel (treatment) agent+additive (Water substitute reagent). The comparison included parameters such as radiation temperature, extinguishing time, and coating performance of the burning fuel.

2. Methods

Synthesis of hydrogel fire extinguishing agents by extracting from water hyacinth has various steps, as shown in Figure 1.

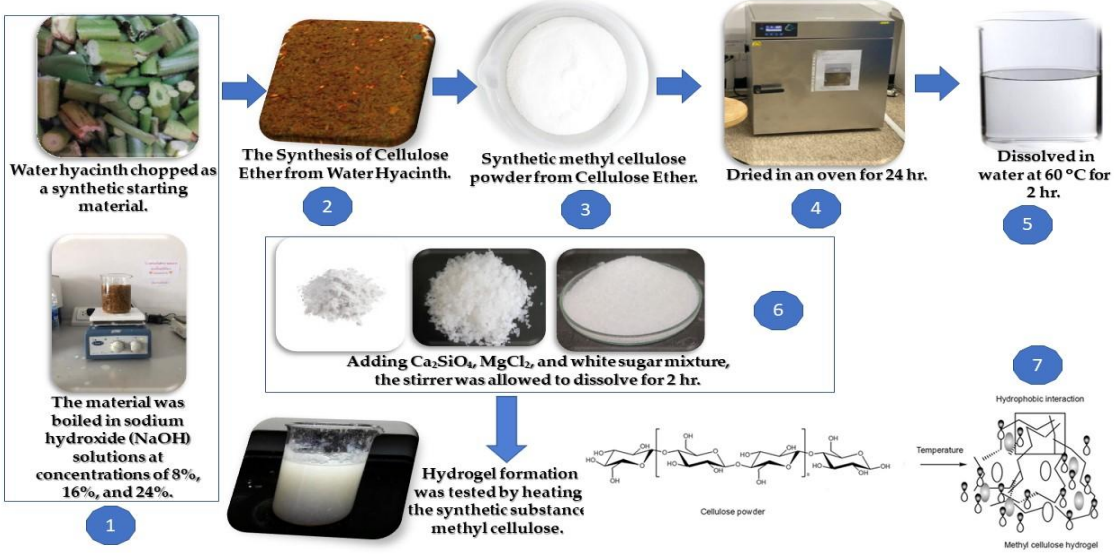

Figure 1 Flow diagram for the production of hydrogel for extinguishing from methyl cellulose

2.1. The Synthesis of Cellulose from Water Hyacinth

Samples of water hyacinth were initially washed thoroughly with clean water. This was followed by washing with distilled water 4- 5 times, sun-drying, and placing in an electric oven at 100°C for 24 hours. After cooling, samples were cut into small pieces and ground into a fine material. The material was boiled in Sodium Hydroxide (NaOH) (Merck, Germany) solutions at concentrations of 8%, 16%, and 24% by weight, each using a volume of 100 ml to extract cellulose. The mixture was boiled for approximately 1 hour until the material was thoroughly softened, and allowed to cool at room temperature. Subsequently, the boiled material was washed four to five times with distilled water to remove the sodium hydroxide, dried at 100°C in an oven for 3 hours, finely ground, and chemically treated as shown in Figure 2A. This was followed by storing in a desiccator to absorb any remaining moisture.

2.2. The Synthesis of Cellulose Ether from Water Hyacinth

A total of 5 grams of cellulose was placed into a 500 ml. beaker, added with 90 ml of isopropyl alcohol (Merck, Germany), and stirred the mixture for 30 minutes. NaOH was added at concentrations of 20%, 25%, and 30% to a volume of 50 ml, and the mixture was stirred for 1 hour. Subsequently, 6, 8, and 10 grams of chloroacetic acid ($C_2H_3ClO_2$) (Merck, Germany) were added, maintaining the temperature at 60°C for 3 hours. The mixture was allowed to cool to room temperature. Acetic acid (CH_3COOH) (Merck, Germany) was added until the solution became neutral. The mixture was filtered and washed with 70% (%v/v) ethanol (Oil Chemical & Supply, Thailand) to obtain cellulose ether, and dried at 60°C for 12 hours. Finally, the samples were stored in a desiccator (Figure 2B).

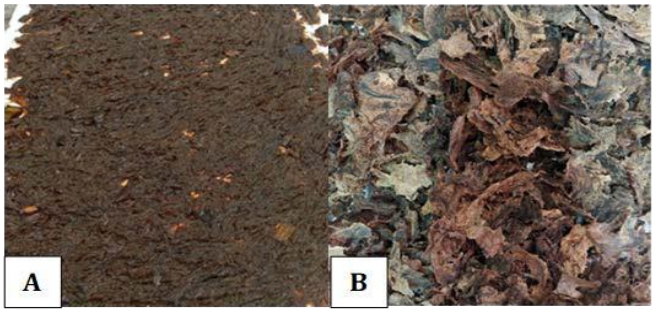

Figure 2 Product from cellulose from simmered water hyacinth finely blended (A), cellulose ether from water hyacinth (B)

2.3. The Synthesis of MC from cellulose ether

A 1.0 mm mesh sieve was used to filter cellulose ether, which was reacted with chloroacetic acid in isopropyl alcohol and 40% sodium hydroxide for 30 minutes. Subsequently, it was dried in an oven at 55°C for 3.5 hours. The liquid portion was removed, and 70% methanol (Oil Chemical & Supply, Thailand) was added to the gel-like portion. Neutralization was performed with 90% citric acid (Merck, Germany) and the pH was tested with litmus paper to ensure neutrality. The gel-like portion was filtered and washed with 70% ethanol for 10 minutes. This process was repeated five more times with methanol and the material was left at room temperature overnight. The outcome was the powdered yield of MC (Figure 3A).

2.4. Testing for Hydrogel Formation

MC powder was dried in an oven for 24 hours to achieve a 1.3% water-by-weight solution. This was followed by the dissolution of MC powder in water at 60°C for 2 hours. Similarly, nanocalcium silicate powder (1wt%) (Merck, Germany) was added to enhance the fluidity of the injection system. Subsequently, Magnesium Chloride (MgCl2) (3 wt%)(Merck, Germany) and white sugar (additive) (1 wt%) (Mitrphol, thailand) were added to the mixture. The mixture was stirred and allowed to dissolve for 2 hours. In this study, hydrogel formation ability was tested in 20 ml of gasoline (PTT,

Thailand) to determine the foaming pattern. This test was used to evaluate the performance of the fuel coating for fire suppression (Figure 3B).

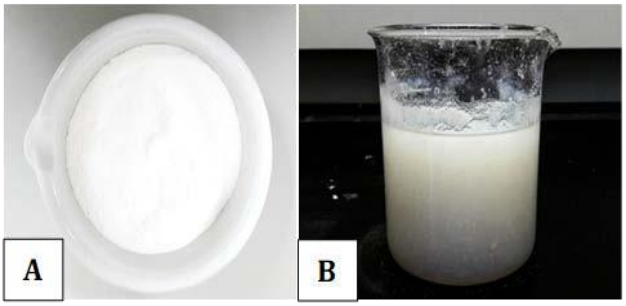

Figure 3 Product from Synthetic MC powder (A), Hydrogel in contact with gasoline (B)

2.5. Performance Testing

2.5.1. FT-IR Analysis

The functional group performance of cellulose hydrogel was analyzed using an FT- IR spectrophotometer with a Nicolet 6700 analyzer (Thermo Scientific, USA). The analysis was conducted over a wavelength range of 400-4000 cm^{-1}.

2.5.2. SEM and Energy Dispersive X-Ray Fluorescence Spectrometer (EDX-FS) Analysis

The morphology of cellulose extract was examined by SEM, JSM-6610 LV, JEOZ (Japan) at an electron energy of 5 Kilovolt (kV). The elemental composition was analyzed using a Shimadzu EDX-FS instrument (Model EDX-8000, Shimadzu, Japan).

2.5.3. Viscosity Analysis

The viscosities of cellulose hydrogel were measured using a viscometer (RVDV-E; AMETEK Brookfield, USA). The test speeds were set at 1, 3, 5, 7, and 10 Revolutions per minute (rpm) using spindle number 5, at temperatures of 20°C and 80°C.

2.5.4. Thermal Property Testing

The thermal properties were analyzed using TGA with a TGA/DSC^{3+} STAR (Mettler Toledo, USA). A sample weighing 10 mg was placed in an alumina crucible and tested in a temperature range of 30-700 °C under a nitrogen gas (Oxytech, Thailand) flow rate of 40 milliliters per minute (ml./min), with a heating rate of 10 Degrees Celsius per minute (°C/min), to determine the decomposition temperature of the sample.

2.5.5. Gel Fraction Analysis

Gel fraction analysis of cellulose hydrogel was conducted by freeze-drying the hydrogel. This was followed by mixing in a solution of 10% sodium hydroxide (NaOH), 5% urea, and 85% distilled water-by-weight at -12°C. The mixture was cycled to separate the insoluble parts, which were dried to determine the gel fraction percentage according to Equation 1.

$$\text{Gel Fraction} = \frac{W_{final}}{W_{initial}} \times 100 \quad (1)$$

where

$W_{initial}$ = Dry weight of original cellulose-hydrogel

W_{final} = Weight of insoluble solids in the mixed solution

2.5.6. Fire Extinguishing Test

Fire extinguishing performance test (Figure 4) was conducted using a standard dry chemical fire extinguisher agent of MAP combined with cellulose powder from water hyacinth in an 80:20 ratio. Meanwhile, a comparison was performed using only 100% MAP. Both samples were filled into 15

pound (lb) fire extinguisher that uses nitrogen gas at 195 psi to propel the chemical powder. The test was conducted using Class B fuel with Fire Rating of 2B. The fuel, namely 25 liters of n-hexane (Merck, Germany), was placed in a square steel tray measuring 676 mm × 676 mm and 6 mm thick. The performance was measured in three aspects. These included 1) thermal radiation values, measured by an infrared thermal camera before and after fire extinguishing, 2) extinguishing time, determining the time from the start to the end of fire extinguishing process, and 3) fire coating performance, evaluating the coating quality on the n-hexane fuel surface.

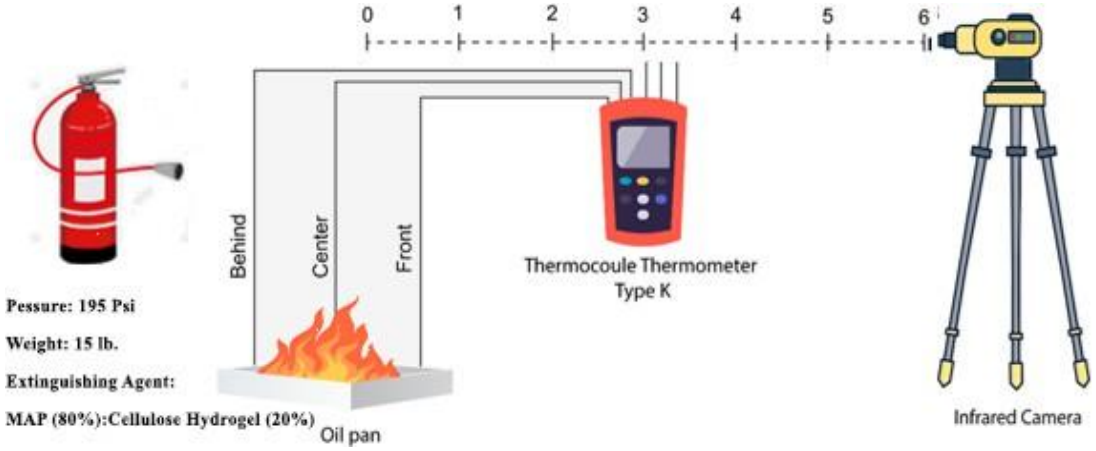

Figure 4 Fire extinguishing performance test and the preparation for fire extinguisher illustration

3. Results and Discussion

3.1. FT-IR Analysis

As shown in Figure 5, distinctive peaks in red circles appeared due to the molecular vibrations of cellulose hydrogel at positions 1,550 from 650 cm^{-1} (Cellulose). These peaks correlate with the characteristic bonds of O-H, C-H, C-O (secondary alcohol), and C-O (primary alcohol) bonds. Additionally, the peak at 1727 cm^{-1} shows the C=O bond found in the hemicellulose structure (Sundari and Ramesh, 2012). The generation of carbonyl groups (C = O) on cellulose surface occurs due to the oxidization of free hydroxyl group.

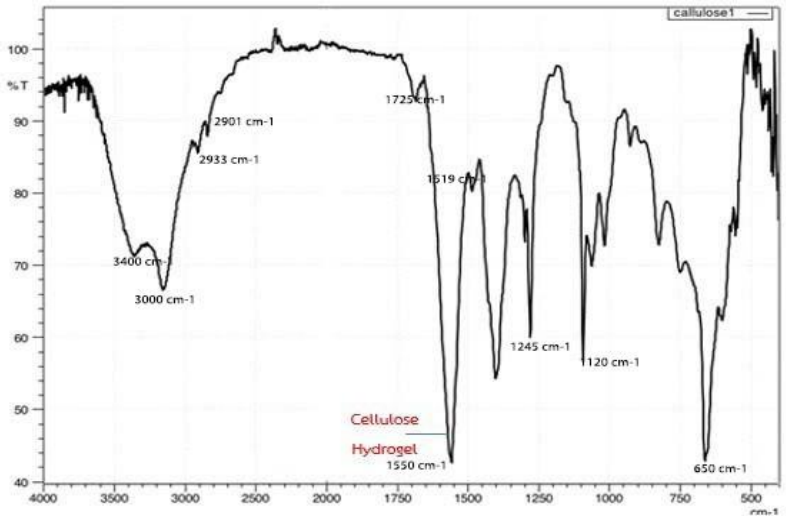

Figure 5 The FT-IR approach is used to analyze the cellulose hydrogel's functional group performance

Consequently, the treated cellulose showed outstanding fire resistance due to its efficient, durable, and restorable flame retardancy mechanism. The peaks at 1519 and 1245 cm^{-1} correspond to the C=C and C-O bonds of the aryl alkyl ether groups in the lignin structures, respectively (Wang et al., 2019). In comparison,

the FT-IR spectrum of cellulose fibers from water hyacinth obtained through chemical processes showed a reduction in the intensity of the peaks at 1727, 1519, and 1245 cm^{-1}. This reduction shows a decrease in the hemicellulose and lignin contents due to the chemical extraction process used on water hyacinth fibers. Additionally, the spectrum correlated with the OH stretching vibration in the 3000-3500 cm^{-1} range, showing the explicit absorption of the hydroxyl groups in MC attributed to their linkage interactions. The C-H stretching vibrations were observed in the 2933-2901 cm^{-1} range and the C-O-C stretching vibration was observed at 1120 cm^{-1}. Figure 6 shows the transition from cellulose powder to hydrogel when exposed to higher temperatures.

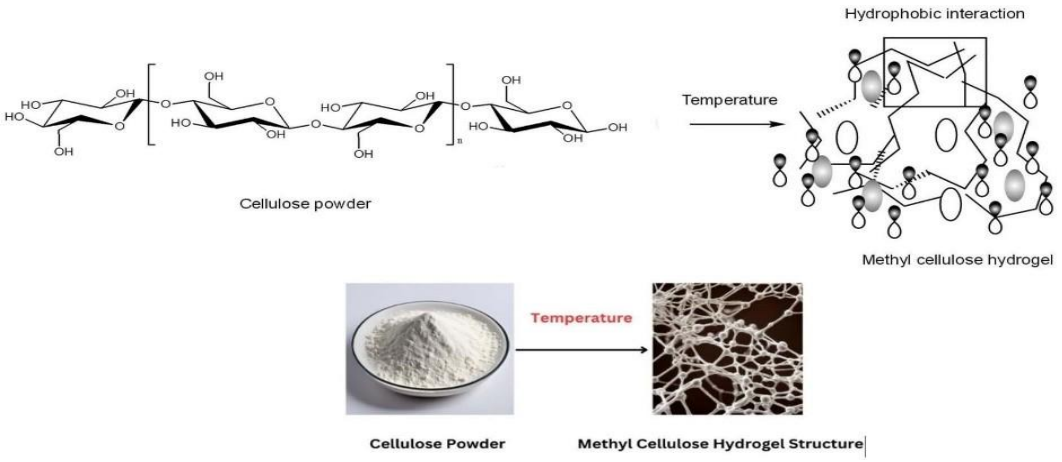

Figure 6 Transformation of Cellulose powder to Cellulose Hydrogel

3.2. Structural model analysis using SEM method of cellulose hydrogel

The isolation of cellulose for the transformation into cellulose ether has been successfully conducted. Crystalline cellulose was obtained as a white powder from water hyacinth (Suryanti et al., 2023). The results of the structural analysis using SEM are shown in Figure 7(A). At a magnification of 5000x, cellulose hydrogel surface consisted of numerous overlapping fibers, consistent with the physical characteristics. Cellulose was completely elongated with fibrils of various lengths and thicknesses at higher magnification. The SEM micrograph showed that the packed fibril structures were separated from each other. Furthermore, MC product showed twisted and blunt flakes which were identical to the commercial MC. Figure 7(B) shows an image at 1000x magnification, indicating the entire cellulose hydrogel as a mass of overlapping fibers. These fibers were dispersed and separated at the micrometer level due to the removal of hemicellulose, lignin, and other substances, causing adhesion during the chemical process (Chandra et al., 2016).

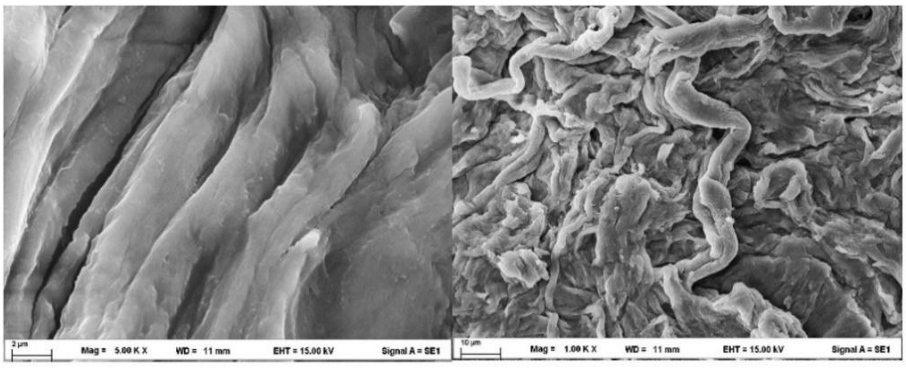

(a) (b)

Figure 7 Characteristic analysis of cellulose hydrogel surface using SEM method at Magnification 5000X (A) and 1000X (B)

3.3. Results of elemental analysis of cellulose hydrogel substances using EDX method

According to the graphic and information from Table 1, the chemical composition analysis of cellulose hydrogel showed the presence of carbon, oxygen, sodium, magnesium, aluminum, silicon, phosphorus, chlorine, and calcium as components (Repon and Mikučionienė, 2021). The proportions of carbon and oxygen were 54.77% and 35.66% respectively, while sodium was at 7.03% (Pullawan et al., 2014).

Table 1 Elemental analysis of cellulose ether using EDX method

Element	Weight %	Atomic %
C	44.53	54.77
O	38.62	35.66
Na	10.94	7.03
Mg	0.32	0.19
Al	0.10	0.06
Si	0.20	0.11
P	0.81	0.38
Cl	2.98	1.24
Ca	1.49	0.55

3.4. Viscosity Analysis

The viscosity of gel was tested at various concentrations with temperatures of 20 and 80°C using a DV-1 digital viscometer (Beijing Jingmeirui Technology Co., Ltd., Beijing, China). The initial temperature at which 50% of fire extinguishing powder turned into a gel was 20°C. When the temperature exceeded 80°C, the gel viscosity increased, with rising temperature. Each sample was measured approximately 2-3 times, and the average values were used as the test results. Subsequently, the viscosity of cellulose solution mixed with borax at different ratios was analyzed and tested at various rotational speeds, with results shown in Figure 8.

According to Figure 8, when the temperature increased from 20°C to 80°C, the viscosity significantly elevated at the higher temperature. At low temperatures, the partial hydroxyl groups in the hydrogel molecular chains form hydrogen bonds between the molecules, leading to chain entanglement at higher temperatures.

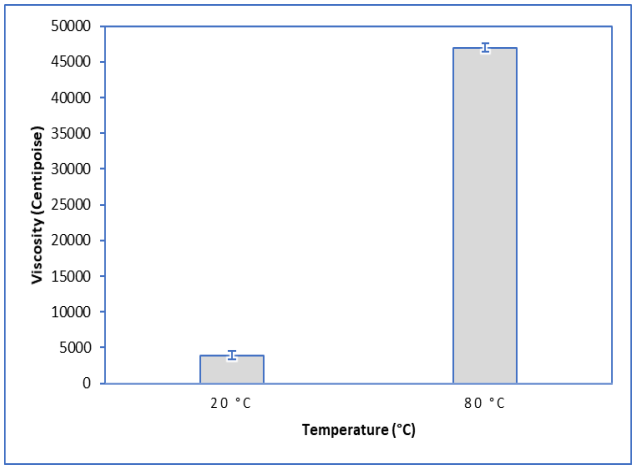

Figure 8 Viscosity of cellulose hydrogel solution at 20°C and 80°C

As the thermal movement of the molecules intensified, the hydrogen bonds between the molecular chains gradually broke down (Peterson et al., 2023), showing the properties of pseudoplastic fluids. Additionally, the amount of NaOH in cellulose solution increases alongside the viscosity. This is because the cross-linking between cellulose chains impedes the flow direction

of the solution. The phenomenon shows an increase in the cross-linking of cellulose chains with the addition of borax. At 20°C, the viscosity of hydrogel slightly increased. After heating to 80°C, the hydrogel transitioned to a sol-gel, with a reduction in flow and an increase in viscosity as the temperature rose (Deng et al., 2014). The increasing viscosity enhanced the adhesion of gel to the surface of Class B fuels, contributing to cooling and preventing oxygen from contacting the fuel heat (Jia et al., 2013). This suggested that the hydrogel enhanced the extinguishing performance of Class B fire.

3.5. Thermal property test

The onset decomposition temperature (T_{onset}), the maximum decomposition temperature (T_{max}), and endset decomposition temperature (T_{endset}) were observed in this study. At temperatures between 300 and 450°C, cellulose decomposition was rapid due to the high mass loss at such temperatures. The percentage of char (% char) at 700°C of cellulose extracted from water hyacinth by the chemical process is shown in Table 2 and Figure 9 A (supplementary).

Table 2 Data from TG and DTG thermograms of cellulose fibers extracted from water hyacinth by the chemical process

Type	T_{onset} (°C)	T_{endset} (°C)	T_{max} (°C)	% char at 700 (°C)
Cellulose-Water Hyacinth (control)	269	349	316	17.2
Cellulose ether	330	380	354	10.3

According to Table 2, the initial and final decomposition temperatures of water hyacinth fibers (control) were found to be 269°C and 349°C, respectively. In comparison, cellulose fibers extracted from water hyacinth by the chemical process showed initial and final decomposition temperatures of 326°C and 375°C, respectively. This difference suggests that water hyacinth fibers have lower initial and final decomposition temperatures than cellulose hydrogel due to the presence of amorphous components such as hemicellulose. Additionally, the char ash percentages of water hyacinth and cellulose fibers extracted from water hyacinth were 17.2% and 10.3%, respectively. Water hyacinth fibers showed a higher char ash content than cellulose hydrogel due to the presence of pyrolytic char from lignin, hemicellulose, and some inorganic substances. This suggests that cellulose fibers obtained by the chemical extraction process were purer, due to the removal of hemicellulose and lignin (Thi et al., 2017).

The thermogram (Figure 9B in supplementary) shows the overlapping decomposition of hemicellulose and lignin. Therefore, a DTG thermogram (Figure 10 in supplementary) was used to determine the decomposition range. Water hyacinth fibers were found to lose their moisture within the range of 41-121°C, with the maximum decomposition temperature in the first stage at 60°C. The second stage included the decomposition of hemicellulose and cellulose within the range of 195-387°C, with a maximum decomposition temperature of 316°C. In comparison, cellulose hydrogel fibers extracted from water hyacinth by the chemical process showed only two stages of decomposition. The first stage occurred within the range of 39-93 °C with a maximum decomposition temperature of 48°C. Meanwhile, the second occurred at 220-402°C with a maximum temperature of 354°C. The results showed that the maximum decomposition temperature in the second stage of cellulose fibers extracted from water hyacinth by the chemical process (354°C) was higher than water hyacinth (316°C). This was due to the reduction of hemicellulose and amorphous components, which possessed lower decomposition temperatures. The decomposition range of cellulose fibers was narrower than water hyacinth, as shown by the narrower second-stage decomposition peak. This is attributed to the reduction in branched structures, including hemicellulose, lignin, and amorphous components, which typically have a broader decomposition range (Leesirisan, 2022).

3.6. Gel Fraction Analysis

As presented in Figure 10 (supplementary), the MC powder extracted from water hyacinth showed increasing gelation behavior with rising temperatures. Initially, at 20°C, cellulose powder passed through gelation at only 2.2%. As the temperature increased incrementally by 50°C, the gelation rate of cellulose powder rose to 17.3%. When the temperature further increased to 80°C, the gelation rate reached 44.6%. The gelation continued to increase with rising temperatures, reaching 98.2% at 140°C. At 200°C, the gelation rate was 99.2%. This behavior is consistent with the viscosity characteristics of the gel, which increases with temperature and enhances adhesion to the fuel surface. The gelation process was proportional to the temperature increase. When the temperature exceeded 200°C, the MC powder sprayed on the fuel surface fully transformed into a gel coating (Huang et al., 2019; Deng et al., 2014).

3.7. Fire Extinguishing Performance Test

Thermal radiation values were measured using a thermal camera, as listed in Tables 3 and 4. The temperature was measured twice for each sample before and after spraying the dry chemical fire extinguisher powder. According to Table 3, thermal radiation before spraying fire extinguisher from both only MAP and MAP+cellulose hydrogel fire-extinguishing agents were not significantly different when comparing the average values from the three tests. However, the temperatures of thermal radiation from the fuel during combustion after spraying only MAP and MAP+ cellulose hydrogel fire-extinguishing agents showed statistically significant differences when comparing the average values of all tests. The average lowest temperature of thermal radiation for MAP+ cellulose hydrogel was 284.67±39.28 seconds, while only MAP was at 368.10±51.46 seconds. Based on gelation analysis of hydrogel, when the fuel temperature exceeds 200°C, cellulose powder transforms into a gel coating the fuel surface more effectively, and showing higher viscosity at elevated temperatures.

Table 3 Temperature values of Thermal Radiation before spraying the dry chemical fire extinguishing powder measured by the Thermal Camera

Test No.	Thermal Radiation temperatures from fuel combustion (℃)		Thermal Radiation temperatures from fuel combustion when spraying fire extinguishing agent (℃)	
	Fire Extinguishing agent: MAP	Fire Extinguishing agent: MAP+Cellulose Hydrogel	Fire Extinguishing agent: MAP	Fire Extinguishing agent: MAP+Cellulose Hydrogel
1.	409.60	496.70	378.30	248.90
2.	504.40	503.60	413.70	326.70
3.	458.90	543.20	312.90	278.40
$\bar{X}$±S.D.	457.63 ± 47.41c	514.50 ± 25.09c	368.10 ± 51.46b	284.67 ± 39.28a

[a,b,c]Different letters indicate statistically significant differences ($P \leq 0.05$)

3.8. Extinguishing Time of Fire Extinguishing Agents

Extinguishing time for Class B fire was measured from the start of spraying the dry chemical fire extinguisher until fire was completely extinguished (Figure 11A in in supplementary). The measurement was performed three times, and the results are listed in Table 4. Based on the results, the average extinguishing time for MAP was 8.70±1.96 seconds, while MAP+ cellulose hydrogel was 4.51±0.97 seconds. The average extinguishing times for the two agents differed significantly. The primary component of the MAP fire extinguishing powder, namely phosphate salts, formed a glass-like layer on the surface of burning solid materials, isolating the fuel from the oxidizing agent. This separation layer was from the thermal decomposition of phosphate salts and the formation of polyphosphates (Li et al., 2019). MAP powder, containing ammonium dihydrogen phosphate ($(NH_4)H_2PO_4$), interfered with the combustion of cellulose materials. Metaphosphoric acid (HPO_3),

with a low melting point, appeared when the powder came into contact with flames, leading to the formation of a glass-like film on solid surfaces and cutting off oxygen contact in Class A fire that burned with glowing embers (Li et al., 2022).

Table 4 Extinguishing Time of Fire Extinguishing Agents for Class B Fire

Test No.	Extinguishing time (Seconds)	
	Fire Extinguishing agent: MAP	Fire Extinguishing agent: MAP+ Cellulose Hydrogel
1.	6.76	3.48
2.	10.67	4.62
3.	8.68	5.43
$\bar{X}\pm$S.D.	8.70 ± 1.96^{b}	4.51 ± 0.97^{a}

^{a,b}Different letters indicate statistically significant differences ($P \leq 0.05$)

This process contributes significantly to fire suppression, with the dry powder showing a cooling effect. The thermal energy required to decompose the dry chemical powder is related to its fire-extinguishing performance. Therefore, all dry chemical agents must be thermally sensitive to react chemically and absorb ("consume") heat. Spraying the dry chemical powder created a dust cloud between the flame and fuel, which facilitated the removal of heat released from the fuel by the flame (Fatsa Fire, 2022).

3.9. Characteristics of Fuel Coating

As presented in Table 5, MAP fire extinguishing agent covered the fuel surface with a yellowish-white powder. MAP+ cellulose hydrogel extinguishing agent also effectively formed a gel-like layer on the fuel surface. This coating functions by burning fuel, cutting off oxygen, and reducing temperature, thereby extinguishing fire (Figure 11 B and C in supplementary).

Table 5 Fire coating characteristics

Test No.	Type of Fire Extinguishing Agents	
	Fire Extinguishing agent: MAP	Fire Extinguishing agent: MAP+ Cellulose Hydrogel
1.	Powder covering Fuel	Gel coating Fuel
2.	Powder covering Fuel	Gel coating Fuel
3.	Powder covering Fuel	Gel coating Fuel

4. Discussion

The study found that cellulose hydrogel extracted from water hyacinth could enhance the effectiveness of extinguishing class B fire, making it more effective than using only MAP. The use of powder extinguishing agents to form hydrogel for extinguishing oil fire is a new method by adding additives to facilitate gel formation on the surface of oil (class B fuel). Thermoresponsive hydrogel possesses unique characteristics due to temperature sensitivity, which addresses the shortcomings of traditional hydrogel. This versatile functional polymer material shows rapid phase behavioral changes when the temperature reaches a specific value (Barros et al., 2014; Ruel-Gariepy and Leroux, 2004), often referred to as the lower critical solution temperature (LCST). In some previous studies, thermoresponsive hydrogel existed in a liquid state below the LCST and solidified into a gel after exceeding the threshold (Dai et al., 2020; Klouda, 2015). The temperature sensitivity of the hydrogel is related to the structures of hydrophilic and hydrophobic groups. At room temperature, hydrogel has high fluidity and low viscosity but rapidly releases water and forms an adhesive layer that coats the surface of the burning materials at high temperatures (Cheng et al., 2017).

Currently, thermoresponsive hydrogel is extensively explored in various fields such as medicine and agriculture (Puspitasari et al., 2022; Lim et al., 2020; Jiang et al., 2018; Chatterjee et al., 2018). For fire- extinguishing applications, hydrogel should show high viscosity and strong adhesion at elevated temperatures. This shows that hydrogel should have significant thermal responsiveness as the phase transition correlates with temperature changes. Most hydrogel used as fire-extinguishing agents is thermally stable, including isopropylacrylamide and MC derivatives (Yang et al., 2016; Hu et al., 2015). Hydrogel containing MC is used to extinguish various types of fire. As the temperature increases, the viscosity begins to rise. At 80 °C, the substance nearly transitions into a gel form, with samples containing a concentration of 5 wt% or higher showing a viscosity greater than 20 Pa.s. In accordance with known information, this study selected 2–8 wt.% solutions as fire-extinguishing agents.

For solutions with concentrations of 2 and 4% by weight, fire extinguishing times were 70 and 74 seconds, respectively. In solutions with concentrations of 6 and 8% by weight, fire extinguishing times were 60 and 115 seconds, respectively (Ma et al., 2021). According to Yu et al. (2016), a scalable process was developed to produce biocompatible hydrogel that could be used to extinguish wildfires. This included using Hydroxymethyl cellulose (HEC) and MC at 1% by weight, supplemented with colloidal silica particles (CSP) at 1% and 5% to deliver the best strength such as long-term stability (no syneresis over one week). The target was achieved with the HEC: MC 80:20 system, regardless of the CSP proportions, by using HEC at a high molecular weight (1.3 MDa) and MC at a low molecular weight (60 kDa). Based on fire tests, various concentrations were used, namely 0.32 wt% HEC, 0.08 wt% MC, and 2 wt% CSPs, with the addition of ammonium polyphosphate (Phos-Chek LC95A). Initially, TGA analysis showed that there was no significant difference in the residue of wood samples coated with only ammonium polyphosphate solution and the hydrogel system (approximately 45 wt%). Under simulated rain conditions, the retardant solution washed away approximately 40 wt% of the initial weight, while the hydrogel retained the retardant substance at 80 wt% (Yu et al., 2016). Based on further studies, Yu et al., (2020) expanded to cover the retardant effects of hydrogel on grass and chip-burning experiments. The results showed that hydrogel could be used as fire barriers for trees, particularly in frequently burned areas, to protect highly preserved plantation areas (Yu et al., 2020).

5. Conclusions

In conclusion, this study found that cellulose hydrogel extracted from water hyacinth could enhance the performance of the MAP + cellulose hydrogel fire-extinguishing agent in extinguishing Class B fire. The hydrogel was more effective than using MAP alone, with a faster extinguishing time of 4.19 seconds. Additionally, the hydrogel could effectively coat Class B fuel surfaces, which reduced the amount of oxygen available for the chain reaction of fire and decreased the Limit Oxygen Index (LOI). It could reduce the heat radiation after spraying MAP+ Cellulose Hydrogel on Class B fire to 284.67°C while spraying only MAP produced a high heat radiation temperature of 368.10°C on Class B fire. This special feature prevented fire from reigniting after being extinguished because of higher temperature was required for self-ignition.

Abbreviations

MC	Methyl Cellulose
FT-IR	Fourier Transform Infrared Spectrometer
SEM	Scanning Electron Microscope
EDX	Energy Dispersive X-Ray Spectroscopy
TGA	Thermogravimetric Analysis
MAP or ABC	Mono-Ammonium Phosphate
Wt%	Weight Percentage
CMC	Carboxymethyl Cellulose
MCC	Microcrystalline Cellulose
CNC	Cellulose Nanocrystals

CNF	Cellulose Nanofibrils
NaHCO3	Sodium Bicarbonate
%	Percentage
NaOH	Sodium Bicarbonate
ml.	Millilitre
°C	Degree Celsius
C2H3ClO3	Chloro Acetic Acid
CH3COOH	Acetic Acid
v/v	Volume per Volume
MgCl2	Magnesium Chloride
cm^{-1}	Centimeter
kV	Kilovolt
rpm	Revolutions Per Minute
mg	Milligram
ml./min	Millilitre Per Minute
°C/min	Celsius Per Minute
lb.	Pound
psi	Pound Per Square Inch
mm.	Millimeter
Tonset	Onset Temperature
Tendset	Endset Temperature
Tmax	Maximum Temperature
TG	Thermogram
DTG	Derivative Thermogram Analysis
NH4H2PO4	Ammonium Dihydrogen Phosphate
HPO3	Metaphosphoric Acid
HEC	Hydroxy Methyl Cellulose
CSP	Colloidal Silica Particles
MDa	Mega Dalton
kDa	Kilo Dalton
LOI	Limit Oxygen Index

Acknowledgements

The authors are grateful to Suan Dusit University and Science Promotion Fund Research and Innovation Fund for funding this study. Science Promotion Fund Research and Innovation Fund, Thailand, Project No. 193094.

Author Contributions

Nuttabodee Viriyawattana: Writing – review & editing, Supervision, Project administration, Methodology, Funding acquisition, Conceptualization. Surachat Sinworn: Writing – review & editing, original draft, Visualization, Methodology, Data curation.

Conflict of Interest

The author(s) declared no potential conflicts of interest regarding the authorship and/or publication of this study.

References

Alavi, M 2019, 'Modifications of microcrystalline cellulose (MCC), nanofibrillated cellulose (NFC), and nanocrystalline cellulose (NCC) for antimicrobial and wound healing applications', *e-Polymers*, vol. 19, no. 1, pp. 103–119, https://doi.org/10.1515/epoly-2019-0013

Bangar, SP, Harussani, MM, Ilyas, RA, Ashogbon, AO, Singh, A, Trif, M & Jafari, SM 2022, 'Surface modifications of cellulose nanocrystals: Processes, properties, and applications', *Food Hydrocolloids*, vol. 130, p. 107689, https://doi.org/10.1016/j.foodhyd.2022.107689

Barros, SC, da Silva, AA, Costa, DB, Cesarino, I, Costa, CM, Lanceros-Méndez, S & Silva, MM 2014, 'Thermo-sensitive chitosan–cellulose derivative hydrogels: swelling behaviour and morphologic studies', *Cellulose*, vol. 21, pp. 4531–4544, https://doi.org/10.1007/s10570-014-0442-9

Boukind, S, Sair, S, Ait Ousaleh, H, Mansouri, S, Zahouily, M, Abboud, Y & El Bouari, A 2022, 'Ambient pressure drying as an advanced approach to the synthesis of silica aerogel composite for building thermal insulation', *Journal of Natural Fibers*, vol. 19, no. 15, pp. 10142–10156, https://doi.org/10.1080/15440478.2021.1993486

Chai, Q, Jiao, Y & Yu, X 2017, 'Hydrogels for biomedical applications: their characteristics and the mechanisms behind them', *Gels*, vol. 3, no. 1, p. 6, https://doi.org/10.3390/gels3010006

Chandra, J, George, N & Narayanankutty, SK 2016, 'Isolation and characterization of cellulose nanofibrils from arecanut husk fibre', *Carbohydrate Polymers*, vol. 142, pp. 158–166, https://doi.org/10.1016/j.carbpol.2016.01.015

Chatterjee, S, Hui, PCL & Kan, CW 2018, 'Thermoresponsive hydrogels and their biomedical applications: Special insight into their applications in textile-based transdermal therapy', *Polymers*, vol. 10, no. 5, p. 480, https://doi.org/10.3390/polym10050480

Cheng, W, Hu, X, Xie, J & Zhao, Y 2017, 'An intelligent gel designed to control the spontaneous combustion of coal: fire prevention and extinguishing properties', *Fuel*, vol. 210, pp. 826–835, https://doi.org/10.1016/J.FUEL.2017.09.007

Dai, M, Shang, Y, Li, M, Ju, B, Liu, Y & Tian, Y 2020, 'Synthesis and characterization of starch ether/alginate hydrogels with reversible and tunable thermoresponsive properties', *Materials Research Express*, vol. 7, no. 8, p. 085701, https://doi.org/10.1088/2053-1591/ab8a0a

Deng, W, Zhang, Q & Wang, Y 2014, 'Catalytic transformations of cellulose and cellulose-derived carbohydrates into organic acids', *Catalysis Today*, vol. 234, pp. 31–41, https://doi.org/10.1016/j.cattod.2013.12.041

Ebara, M, Kotsuchibashi, Y, Narain, R, Idota, N, Kim, YJ & Hoffman, JM 2014, 'Smart hydrogels', *Smart Biomaterials*, vol. 1, pp. 9–65, https://doi.org/10.1007/978-4-431-54400-5_2

Evegren, F & Hertzberg, T 2017, 'Fire safety regulations and performance of fibre-reinforced polymer composite ship structures', *Proceedings of the Institution of Mechanical Engineers, Part M: Journal of Engineering for the Maritime Environment*, vol. 231, no. 1, pp. 46–56, https://doi.org/10.1177/1475090215620449

Fatsa Fire 2022, 'Most effective fire extinguishing methods', *Fatsa Fire*, viewed 26 September 2022, (https://www.fatsafire.com/most-effective-fire-extinguishing-methods/)

Han, Z, Gong, L, Du, Z & Duan, H 2020, 'A novel environmental-friendly gel dry-water extinguishant containing additives with efficient combustion suppression efficiency', *Fire Technology*, vol. 56, no. 6, pp. 2365–2385, https://doi.org/10.1007/s10694-020-00957-3

Harahap, M, Daulay, N, Zebua, D & Gea, S 2023, 'Nanofiber cellulose/lignin from oil palm empty fruit bunches and the potential for carbon fiber precursor prepared by wet-spinning', *International Journal of Technology*, vol. 14, no. 1, pp. 152–161, https://doi.org/10.14716/ijtech.v14i1.5082

Hu, X, Cheng, W, Nie, W & Shao, Z 2015, 'Synthesis and characterization of a temperature-sensitive hydrogel based on sodium alginate and N-isopropylacrylamide', *Polymers for Advanced Technologies*, vol. 26, no. 11, pp. 1340–1345, https://doi.org/10.1002/pat.3682

Huang, Z, Yan, L, Zhang, Y, Gao, Y, Liu, X, Liu, Y & Li, Z 2019, 'Research on a new composite hydrogel inhibitor of tea polyphenols modified with polypropylene and mixed with halloysite nanotubes', *Fuel*, vol. 253, pp. 527–539, https://doi.org/10.1016/j.fuel.2019.03.152

Jamsaz, A & Goharshadi, EK 2023, 'Graphene-based flame-retardant polyurethane: A critical review', *Polymer Bulletin*, vol. 80, no. 11, pp. 11633–11669, https://doi.org/10.1007/s00289-023-04719-y

Jia, X, Chen, Y, Shi, C, Ye, Y, Wang, P, Zeng, X & Wu, T 2013, 'Preparation and characterization of cellulose regenerated from phosphoric acid', *Journal of Agricultural and Food Chemistry*, vol. 61, no. 50, pp. 12405–12414, https://doi.org/10.1021/jf4042358

Jiang, P, Cheng, Y, Yu, S, Lu, J & Wang, H 2018, 'Study on the effect of 1-butanol soluble lignin on temperature-sensitive gel', *Polymers*, vol. 10, no. 10, p. 1109, https://doi.org/10.3390/polym10101109

Kabiri, K, Omidian, H & Zohuriaan-Mehr, MJ 2003, 'Novel approach to highly porous superabsorbent hydrogels: synergistic effect of porogens on porosity and swelling rate', *Polymer International*, vol. 52, no. 7, pp. 1158–1164, https://doi.org/10.1002/pi.1218

Kibar, EA & Us, F 2014, 'Evaluation of structural properties of cellulose ether-corn starch based biodegradable films', *International Journal of Polymeric Materials and Polymeric Biomaterials*, vol. 63, no. 7, pp. 342–351, https://doi.org/10.1080/00914037.2013.845190

Klouda, L 2015, 'Thermo responsive hydrogels in biomedical applications: A seven-year update', *European Journal of Pharmaceutics and Biopharmaceutics,* vol. 97, pp. 338–349, https://doi.org/10.1016/j.ejpb.2015.05.017

Leesirisan, S 2022, 'Properties of pineapple-leaf fibers after chemical treatments', *Bulletin of Applied Sciences*, vol. 7, no. 7, pp. 25–31

Li, H, Fenf, L, Du, D, Guo, X, Hua, M & Pan, X 2019, 'Fire suppression performance of a new type of composite superfine dry powder', *Fire Materials,* vol. 43, pp. 905–916, https://doi.org/10.1002/fam.2750

Li, Y, Qi, L, Liu, Y, Qiao, J, Wang, M, Liu, X & Li, S 2022, 'Recent advances in halogen-free flame retardants for polyolefin cable sheath materials', *Polymers,* vol. 14, article 2876, https://doi.org/10.3390/polym14142876

Lim, JW, Kim, HJ, Kim, Y, Shin, SG, Cho, S, Jung, WG & Jeong, JH 2020, 'An active and soft hydrogel actuator to stimulate live cell clusters by self-folding', *Polymers,* vol. 12, no. 3, article 583, https://doi.org/10.1126/science.abh4357

Ma, L, Huang, X, Sheng, Y, Liu, X & Wei, G 2021, 'Experimental study on thermosensitive hydrogel used to extinguish class A fire', *Polymers,* vol. 13, no. 3, pp. 1–14, https://doi.org/10.3390/polym13030367

Ma, X, Chang, PR & Yu, J 2008, 'Properties of biodegradable thermoplastic pea starch/carboxymethyl cellulose and pea starch/microcrystalline cellulose composites', *Carbohydrate Polymers,* vol. 72, no. 3, pp. 369–375, https://doi.org/10.1016/j.carbpol.2007.09.002

Nugroho, PS, Latief, Y & Wibowo, W 2022, 'Structural equation modelling for improving fire safety reliability through enhancing fire safety management on high-rise building', *International Journal of Technology,* vol. 13, no. 4, pp. 740–750, https://doi.org/10.14716/ijtech.v13i4.5517

Nurhayati, Irianto, HE, Riastuti, R, Pangesty, AI, Nugraha, AF, Todo, M, Jumahat, A & Chalid, M 2024, 'Extraction and characterization of micro-fibrillated cellulose from rice husk waste for biomedical purposes', *International Journal of Technology,* vol. 15, no. 2, pp. 342–352, https://doi.org/10.14716/ijtech.v15i2.6698

Peterson, JD, Zou, W, Larson, RG & Cates, ME 2023, 'Wormlike micelles revisited: A comparison of models for linear rheology', *Journal of Non-Newtonian Fluid Mechanics,* vol. 322, article 105149, https://doi.org/10.1016/j.jnnfm.2023.105149

Pullawan, T, Wilkinson, AN, Zhang, LN & Eichhorn, SJ 2014, 'Deformation micromechanics of all-cellulose nanocomposites: Comparing matrix and reinforcing components', *Carbohydrate Polymers,* vol. 100, pp. 31–39, https://doi.org/10.1016/j.carbpol.2012.12.066

Puspitasari, D, Budhijanto, W, Purnomo, E & Nugraheni, PS 2022, 'Optimization of Irgacure® 2959 concentration as photo-initiator on chitosan-alginate based hydrogel for colon tissue sealant', *International Journal of Technology,* vol. 13, no. 8, pp. 1704–1714, https://doi.org/10.14716/ijtech.v13i8.6164

Qin, B, Lu, Y, Li, Y & Wang, D 2014, 'Aqueous three-phase foam supported by fly ash for coal spontaneous combustion prevention and control', *Advanced Powder Technology,* vol. 25, no. 5, pp. 1527–1533, https://doi.org/10.1016/j.apt.2014.04.010

Rahman, MS, Hasan, MS, Nitai, AS, Nam, S, Karmakar, AK, Ahsan, MS & Ahmed, MB 2021, 'Recent developments of carboxymethyl cellulose', *Polymers,* vol. 13, no. 8, article 1345, https://doi.org/10.3390/polym13081345

Repon, MR & Mikučionienė, D 2021, 'Progress in flexible electronic textile for heating application: A critical review', *Materials*, vol. 14, no. 21, article 6540, https://doi.org/10.3390/ma14216540

Ruel-Gariepy, E & Leroux, JC 2004, 'In situ-forming hydrogels—review of temperature-sensitive systems', *European Journal of Pharmaceutics and Biopharmaceutics*, vol. 58, no. 2, pp. 409–426, https://doi.org/10.1016/j.ejpb.2004.03.019

Sayara, T & Sánchez, A 2019, 'A review on anaerobic digestion of lignocellulosic wastes: Pretreatments and operational conditions', *Applied Sciences*, vol. 9, no. 21, p. 4655, https://doi.org/10.3390/app9214655

Sen, S, Singh, A, Bera, C, Roy, S & Kailasam, K 2022, 'Recent developments in biomass derived cellulose aerogel materials for thermal insulation application: A review', *Cellulose,* vol. 29, no. 9, pp. 4805–4833, https://doi.org/10.1007/s10570-022-04586-7

Shi, B & Zhou, F 2014, 'Impact of heat and mass transfer during the transport of nitrogen in coal porous media on coal mine fires', *The Scientific World Journal*, vol. 2014, no. 1, pp. 1–9, https://doi.org/10.1155/2014/293142

Shi, Q & Qin, B 2019, 'Experimental research on gel-stabilized foam designed to prevent and control spontaneous combustion of coal', *Fuel,* vol. 254, pp. 1–10, https://doi.org/10.1016/j.fuel.2019.05.141

Sundari, MT & Ramesh, A 2012, 'Isolation and characterization of cellulose nanofibers from the aquatic weed water hyacinth—Eichhornia crassipes', *Carbohydrate Polymers,* vol. 87, no. 2, pp. 1701–1705, https://doi.org/10.1016/j.carbpol.2011.09.076

Suryanti, V, Kusumaningsih, T, Safriyani, D & Cahyani, IS 2023, 'Synthesis and characterization of cellulose ethers from screw pine (*Pandanus tectorius*) leaves cellulose as food additives', *International Journal of Technology*, vol. 14, no. 3, pp. 659–668, https://doi.org/10.14716/ijtech.v14i3.5288

Thi, BTN, Ong, LK, Thi, DTN & Ju, YH 2017, 'Effect of subcritical water pretreatment on cellulose recovery of water hyacinth (*Eichhornia crassipe*)', *Journal of the Taiwan Institute of Chemical Engineers*, vol. 71, pp. 55–61, https://doi.org/10.1016/j.jtice.2016.12.028

Varma, RS 2019, 'Biomass-derived renewable carbonaceous materials for sustainable chemical and environmental applications', *ACS Sustainable Chemistry & Engineering*, vol. 7, no. 7, pp. 6458–6470, https://doi.org/10.1021/acssuschemeng.8b06550

Viriyawattana, N & Sinworn, S 2023, 'Performance improvement of the dry chemical-based fire extinguishers using nanocalcium silicate synthesized from biowaste', *Journal of Fire Sciences*, vol. 41, no. 3, pp. 73–88, https://doi.org/10.1177/07349041231168553

Wang, D, Dou, G, Zhong, X, Xin, H & Qin, B 2014, 'An experimental approach to selecting chemical inhibitors to retard the spontaneous combustion of coal', *Fuel*, vol. 117, pp. 218–223, https://doi.org/10.1016/j.fuel.2013.09.070

Wang, Z, Yao, Z, Zhou, J, He, M, Jiang, Q, Li, S, Ma, Y, Liu, M & Luo, S 2019, 'Isolation and characterization of cellulose nanocrystals from *Pueraria* root residue', *International Journal of Biological Macromolecules*, vol. 129, pp. 1081–1089, https://doi.org/10.1016/j.ijbiomac.2018.07.055

Xi, Z, Jiang, M, Yang, J & Tu, X 2014, 'Experimental study on advantages of foam–sol in coal dust control', *Process Safety and Environmental Protection*, vol. 92, no. 6, pp. 637–644, https://doi.org/10.1016/j.psep.2013.11.004

Yadav, A, de Souza, FM, Dawsey, T & Gupta, RK 2022, 'Recent advancements in flame-retardant polyurethane foams: A review', *Industrial & Engineering Chemistry Research*, vol. 61, no. 41, pp. 15046–15065, https://doi.org/10.1021/acs.iecr.2c02670

Yang, C & Lü, X 2021, 'Composition of plant biomass and its impact on pretreatment', in *Advances in 2nd Generation of Bioethanol Production*, pp. 71–85, Woodhead Publishing, https://doi.org/10.1016/B978-0-12-818862-0.00002-9

Yang, Y, Zhu, H, Tsai, Y, Bai, L & Deng, J 2016, 'Study on the thermal stability of thermosensitive hydrogel', *Procedia Engineering*, vol. 135, pp. 501–509, https://doi.org/10.1016/j.proeng.2016.01.162

Yu, AC, Chen, H, Chan, D, Agmon, G, Stapleton, LM, Sevit, AM, Tibbitt, MW, Acosta, JD, Zhang, T, Franzia, PW, Langer, R & Appel, EA 2016, 'Scalable manufacturing of biomimetic moldable hydrogels for industrial applications', *PNAS*, vol. 113, no. 50, pp. 14255–14260, https://doi.org/10.1073/pnas.1618156113

Yu, AC, Lopez Hernandez, H, Kim, AH, Stapleton, LM, Brand, RJ, Mellor, ET, Bauer, CP, McCurdy, GD, Wolff, AJ III, Chan, D, Criddle, CS, Acosta, JD & Appel, EA 2020, 'Wildfire prevention through prophylactic treatment of high-risk landscapes using viscoelastic retardant fluids', *PNAS*, vol. 116, no. 42, pp. 20820–20827, https://doi.org/10.1073/pnas.1907855116

Yuan, J, Zhu, J, Bi, H, Meng, X, Liang, S, Zhang, L & Wang, X 2013, 'Graphene-based 3D composite hydrogel by anchoring Co_3O_4 nanoparticles with enhanced electrochemical properties', *Physical Chemistry Chemical Physics*, vol. 15, no. 31, pp. 12940–12945, https://doi.org/10.1039/C3CP51710A

Zhang, Y, Tian, Z, Ye, Q & Lu, Y 2023, 'Research progress of gel foam extinguishing agent in coal mines', *Fire*, vol. 6, no. 12, p. 470, https://doi.org/10.3390/fire6120470